

The focusing and collimation effects of Cold atomic clouds passing through a Gaussian beam

Zhenglu Duan^{1,3*}, Shuyu Zhou^{2†}, Tao Hong², Yuzhu Wang², and Weiping Zhang^{3‡}

¹*College of Physics and Communication Electronics,
Jiangxi Normal University, Nanchang, 330022, China*

²*Key Laboratory for Quantum Optics, Shanghai Institute of Optics and Fine Mechanics,
The Chinese Academy of Sciences, Shanghai 201800, China and*

³*State Key Laboratory of Precision Spectroscopy, Department of physics,
East Normal University of China, Shanghai 20062, China*

We have demonstrated an atom-optical lens, with the advantage of a small scale and flexible adjustment of the parameters, created by far red-detuned Gaussian laser beam perpendicular to the propagation direction of the cold atomic cloud. This work presents the focusing and collimation effect of a cold atomic cloud, with uniform translational velocity and with vanishing initial translational velocity in gravity respectively, by the atom-optical lens. The object-image relation, focal length and the collimation effect of the atom-optical lens have been analyzed both theoretically and experimentally.

PACS numbers: 03.75.Be, 37.10.Vz

I. INTRODUCTION

With the development of laser cooling and evaporative cooling techniques, it is easy to obtain ultracold atomic clouds at the temperature order of $1\mu\text{K}$ [1–3]. This kind of ultralow temperature atomic cloud is suitable as a medium in atom optics studies [4, 5]. Atom-optical lens is one of the fundamental atom-optical elements, which can focus, collimate, image and transmit the atom beam. Therefore it has been implemented in many ways, such as, atom lithography, atom interferometry and atom interference. Up to now two kinds of atomic lens, based on magnetic or far-detuned optical fields, have been developed. Focusing has been achieved through magnetic lenses [6–9]. Atom-optical lens based on magnetic fields are advantageous for coherent atom-optic research owing to their extremely high optical quality. The focusing dynamics have also been investigated with magnetic atomic lens; specifically, the isotropic three-dimensional (3D) focusing of atoms with a single-impulse magnetic lens [10]. However, it is difficult to build flexible optical systems because magnetic atom-optical elements have a large scale. Laser beams are often used to build atom-optical lens because of their interaction with atoms [11]. They have a small scale and is flexible to realize the combination of atomic lenses. For example, atom-optical lenses can be achieved through red-detuned Gaussian beams or blue-detuned doughnut beams [5, 12–16]. There are other ways to achieve an atom-optical lens, such as by the use of radiation-pressure force [19, 20], near-field light [21, 22], and far-detuned and resonant standing wave fields [23]. A focused Gaussian laser beam with red detuning also

can be used as an atom-optical lens. Early experiments demonstrated this kind of atomic beams focusing using the dipole force [5, 12, 13, 24, 25]. The focusing dynamics of a trapped BEC interacting with laser pulses have also been investigated [26]. Aberration-free atom-optical lenses based on the optical dipole force have also been proposed [27, 28]. Heating and cooling effects caused by an adiabatic compression and expansion when the cold atomic cloud is close to or far from the focus of the Gaussian beam, respectively, have likewise been found [31].

In previous work we have numerically and experimentally studied the ultracold atomic cloud and BEC wave packet passing through focused red-detuned Gaussian laser beam [32]. The focusing, advancement and one-dimensional collimation effects have been observed, which agreed with the numerical simulation results. Specially, the one-dimensional collimation effect of wave cloud is interesting because it is very useful in many important aspects required low divergence sources, such as atom lithography, atom interferometry, atomic fountain cloud, atomic physics collision experiments, ultra high resolution optical spectrum, quantum frequency standard and atom interference. One method of producing such highly collimated beams is using one-dimensional cooling technology [33]. Another one-dimensional collimation method is also realized when atomic beam through atomic lens based on magnetic field [34]. Our method, however, has the advantage of small scale and flexible adjustment of the parameters of the atomic lens.

In this work the object-image relation and the collimation of the atom-optical lens created by the far red-detuned Gaussian beams are studied theoretically and experimental. This work is helpful to further understand the properties of atom-optical lens and one-dimensional collimation effect of atomic cloud without cooling.

The paper is organized as follows. In sec. II we first investigate the optical properties, such as object-image relation, focal length of atomic lens induced by far

[1] * E-mail: duanzhenglu@tsinghua.org.cn

[2] † E-mail: syz@siom.ac.cn

[3] ‡ E-mail: wpzhang@phy.ecnu.edu.cn

red-detuned Gaussian laser beam using particle tracing method when the atom is with uniform velocity and under gravity field, respectively. In Sec. III the collimation effect is analytically studied, and then the numerical simulation is used to verify the valid of the analytical results. In Sec. IV the experimentally studying of the focusing, imaging and collimation effect is also presented and discussed. Finally we conclude the work.

II. THEORY AND NUMERICAL ANALYSIS

In Figure 1, we consider a cold atomic cloud with initial temperature T_0 located at the position $(0, 0, L_o)$. When the atomic cloud with initial translational velocity v_{z_0} propagates along z axes to a far red-detuned focused Gaussian laser beam, the atomic cloud undergoes enough free expansion that the position of every atoms in the cloud is correlated with its velocity distribution. The potential induced by the laser beam has the following form:

$$U = U_0 \exp\left(-\frac{y^2 + z^2}{\sigma_0^2}\right), \quad (1)$$

where $U_0 = \hbar\Omega_0^2/4(\delta + i\gamma/2)$. Here Ω_0 is determined by the intensity in the center of the Gaussian beam, and σ_0 is the waist width of the Gaussian beam. $\delta = \omega_L - \omega_a$ presents the detuning between the laser frequency and the transition frequency of the atom, and γ represents the decay rate of the atomic excited state owing to spontaneous radiation. When the detuning is red, the potential is negative and presents an attractive force when the atoms passing through it. The red-detuned Gaussian laser beam can therefore serve as a focal cylindrical atomic lens.

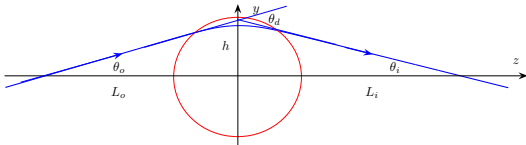


FIG. 1: (Color online) Atomic trajectory when the atom passing through the Gaussian laser beam.

Now we will investigate the optical properties of the atomic lens, such as object-image relation, focal length and aberration, by solving the motion equation of atoms:

$$m \frac{d^2}{dt^2} \vec{r} = -\frac{\partial}{\partial \vec{r}} U, \quad (2)$$

where m is the atom mass.

A. Object-Image relation

Because nonlinear coupling Eq. (2) is difficult to solve, without loss of physics, we assume that the incident kinetic energy $E_0 = mv_{z_0}^2/2 \gg U$, so the velocity along z direction is almost not changed in the process, i.e., $v_z(t) \simeq v_{z_0}$. Now, the potential can be expressed as

$$U = U_0 \exp\left(-\frac{y^2}{\sigma_0^2}\right) \exp\left(-\frac{(v_{z_0}t - L_o)^2}{\sigma_0^2}\right). \quad (3)$$

Substituting Eq. (3) into equation (2) one obtains

$$m\ddot{x} = 0 \quad (4a)$$

$$m\ddot{y} = F_y(t) \quad (4b)$$

$$m\ddot{z} = 0 \quad (4c)$$

where

$$F_y(t) = \frac{2yU_0}{\sigma_0^2} \exp\left(-\frac{y^2}{\sigma_0^2}\right) \exp\left(-\frac{(v_{z_0}t - L_o)^2}{\sigma_0^2}\right). \quad (5)$$

Eq.(4) shows that the motion of atoms in different directions is decoupled. The motion of atoms in central attractive force now reduces to the motion of the atom under the time dependent force along y direction. Owing to no interaction happened along x direction in our model, hereafter transverse direction only means y direction.

From Fig. 1 one observes that the deflection angle of atom passing through laser beam relates with the change of velocity of the atom along y direction.

The momentum change along y direction can be found with the law of impulse-momentum

$$m\Delta v_y = \int_{-\infty}^{\infty} F_y(t) dt. \quad (6)$$

We assume the shift of the atom in the effective interaction range $r \leq \sigma_0$ (see Fig. 1) along y direction is almost not changed, so the integral of Eq. (6) gives

$$m\Delta v_y = \frac{2\sqrt{\pi}hU_0}{\sigma_0 v_{z_0}} \exp\left(-\frac{h^2}{\sigma_0^2}\right), \quad (7)$$

where h is distance of the atom trajectory from the z axial.

Considering $E_0 \gg U$, the deflection angle $\theta_d \ll 1$, and

$$\begin{aligned} \theta_d &\simeq \frac{|\Delta v_y|}{v_{z_0}} \\ &= \frac{\sqrt{\pi}h|U_0|}{\sigma_0 E_0} \exp\left(-\frac{h^2}{\sigma_0^2}\right). \end{aligned} \quad (8)$$

Under paraxial approximation, i.e., $h \ll \sigma_0, L_o, L_i$, the incident and exit angles, respectively, are

$$\theta_o \simeq \frac{h}{L_o} \quad (9a)$$

$$\theta_i \simeq \frac{h}{L_i} \quad (9b)$$

and Eq. (8), keeping to first order, can be rewritten as

$$\theta_d = \frac{\sqrt{\pi}h|U_0|}{\sigma_0 E_0}. \quad (10)$$

According to $\theta_d = \theta_o + \theta_i$, one gets

$$\frac{\sqrt{\pi}|U_0|h}{\sigma_0 E_0} = \frac{h}{L_i} + \frac{h}{L_o}. \quad (11)$$

If we define the focal length as

$$f = \frac{E_0 \sigma_0}{\sqrt{\pi}|U_0|}. \quad (12)$$

Eq. (11) becomes

$$\frac{1}{f} = \frac{1}{L_i} + \frac{1}{L_o}, \quad (13)$$

which is just the Gaussian formula of thin-lens in light-ray optics. We refer Eq. (13) as Gaussian formula of atomic optics.

B. In gravity field

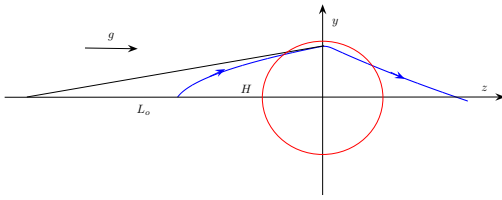


FIG. 2: (Color online) Atomic trajectory when the atom passing through the Gaussian laser beam in the gravity.

In this part we will consider an atom released from the position $(0, 0, H)$ with a vanishing initial vertical velocity and then falls through the focused Gaussian laser beam under the gravity. According to the law of conservation of energy, at the height equal to the center of laser beam, the vertical kinetic energy of the atom is

$$\begin{aligned} E_0 &= \frac{1}{2}mv_{z_0}^2 \\ &= mgH. \end{aligned} \quad (14)$$

In gravity field case, therefore, the focal length of the atomic lens is written as

$$f = \frac{mgH\sigma_0}{\sqrt{\pi}|U_0|}. \quad (15)$$

Assuming the atom reaches the maximal transverse distance h after time t_0 and then flies back and crosses the z axial again after time t_i , the following relation holds

$$\begin{aligned} h &= t_0 v_{y0} \\ &= t_i |v_{yg}|, \end{aligned} \quad (16)$$

where v_{y0} and v_{yg} are the initial and transverse velocities after the atom passing through the laser beam, respectively.

Likewise, keeping to first order, Eq. (7) can be rewritten as

$$v_{yg} - v_{y0} = -\frac{v_{z_0}h}{f}. \quad (17)$$

Combining Eqs. (16) and (17) one finds the time t_i expressed as

$$t_i = \frac{t_0}{\frac{v_{z_0}}{f}t_0 - 1}. \quad (18)$$

The falling distance after the atom flies back and reaches the z -axial again is

$$\begin{aligned} H_i &= v_{z_0}t_i + \frac{1}{2}gt_i^2 \\ &= 2H \frac{f}{2H-f} \left(1 + \frac{f}{4H-2f} \right). \end{aligned} \quad (19)$$

Defining effective image distance $L_{ig} = H_i / \left(1 + \frac{f}{4H-2f} \right)$ and effective object distance $L_{og} = 2H$, Eq. (19) can be rewritten as

$$\frac{1}{f} = \frac{1}{L_{ig}} + \frac{1}{L_{og}}, \quad (20)$$

which is similar with Eq. (13) and called the object-image relation of atomic lens in the gravity.

Obviously, in the gravity case, the object and image distance is not the real falling distance. If one wants to experimentally observe the minimal focused spot of the atomic cloud by absorption image technology, the probe laser beam should be located at H_i and record the signal after time $t_o + t_i$.

III. COLLIMATION EFFECT

Collimation of atomic beam is very useful for nanolithography, atom interferometry and gravity-gradiometer, and cold collision studies. Now the well collimated atomic beam can be obtained by nozzles, transverse cooling, atomic lens. In this section, however, we theoretically study the collimation effect of the atomic cloud passing through the Gaussian beam.

A. Uniform velocity

To begin with, we investigate the collimation effect when the atomic cloud with the initial temperature T_0 has a uniform initial center velocity without gravity. This is a good approximation when the initial center velocity of the atomic cloud is large enough.

Different from the case of transverse cooling, atomic lens can not only collimate, but focus the atomic cloud, so in this paper we use the velocity spread of the atomic cloud to measure the collimation instead of the angular divergence.

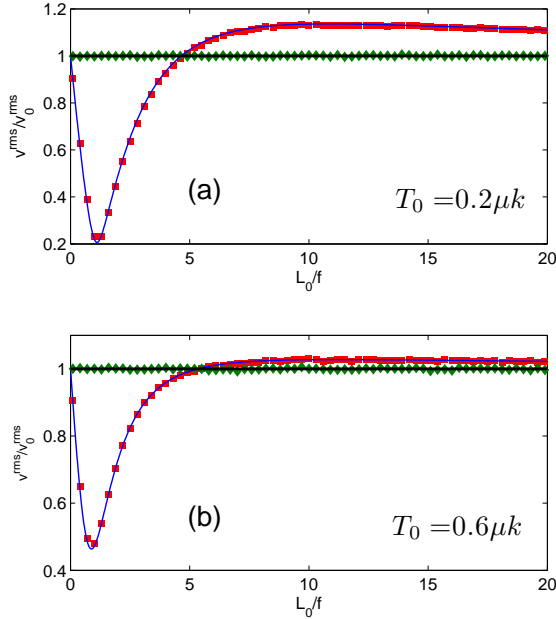


FIG. 3: (Color online) Transverse velocity spread as function of object distance at different initial temperature. The thin and thick solid lines represent the transverse and vertical velocity spread given by Eqs. (23) and (27). The symbol \blacklozenge and \blacksquare represent the corresponding simulation results. In the simulation the initial radial and velocity of the atomic cloud respectively are $R_0 = 0.1\mu\text{m}$, and $v_{z0} = 0.3\text{ms}^{-1}$. The parameters for the optical potential respectively are $U_0 = -20 \times 10^{-29}\text{J}$, $\sigma_0 = 30\mu\text{m}$.

Based on the geometric relation in Fig. 1, one has

$$\frac{h}{L_o} \simeq \frac{v_{y0}}{v_{z0}}. \quad (21)$$

Combining Eqs. (7) and (21), the velocity v_y of the atom deflected by the laser beam along y direction is given by the following expression:

$$v_y = v_{y0} \left[1 - \frac{L_o}{f} \exp\left(-\frac{v_{y0}^2}{\Delta v_0^2}\right) \right], \quad (22)$$

where $\Delta v_0 = v_{z0} \sigma_0 / L_o$.

Then we find the root-mean-square (RMS) velocity along y direction of the atomic cloud passing through the laser beam

$$\begin{aligned} (v_y^{rms})^2 &= A \int_{-\infty}^{\infty} v_{y0}^2 \left[1 - \frac{L_o}{f} \exp\left(-\frac{v_{y0}^2}{\Delta v_0^2}\right) \right]^2 \\ &\quad \times \exp\left(-\frac{mv_{y0}^2}{2k_B T_0}\right) dv_{y0} \\ &= \left(\frac{1}{(2\alpha + 1)^{3/2}} \frac{L_o^2}{f^2} - 2 \frac{1}{(\alpha + 1)^{3/2}} \frac{L_o}{f} + 1 \right) (v_0^{rms})^2, \end{aligned} \quad (23)$$

where $A = \sqrt{m/2\pi k_B T_0}$ with Boltzmann constant k_B , $\alpha = \sigma_a^2 / \sigma_0^2$ with $\sigma_a^2 = 2k_B T_0 L_o^2 / mv_{z0}^2$ the size of the atomic cloud when it reaches the laser beam center, and $v_0^{rms} = \sqrt{k_B T_0 / m}$ the initial RMS velocity of the atomic cloud. One can see that the parameter α can denote the degree of paraxial approximation.

Fig. 4 shows the transverse RMS velocity (thin solid lines) as function of the object distance. We find that the transverse RMS velocity first decreases, then increases and finally decreases and asymptotically tends to initial one with increasing the object distance. Obviously, there exists a region in which the transverse RMS velocity is smaller than the initial one. This phenomenon can be interpreted that, when the object distance is very short, the size of the atomic cloud σ_a is far smaller than the waist of laser beam σ_0 , i.e., $\alpha \ll 1$, therefore the paraxial approximation is well satisfied. Under this condition the laser beam can be viewed as an ideal lens, and Eq. (23) is reduced to $v_y^{rms} \simeq |L_o/f - 1| v_0^{rms}$. So the velocity spread first decreases and then increases with increasing the object distance. When the object distance continuously increases, $\alpha \ll 1$, or the paraxial approximation is not well satisfied, the aberration effect becomes significant. The deflection angle of hot atom is less than that of those cool atoms. The total effect is that, involving the aberration, the transverse RMS velocity is smaller than the ideal one. If the object distance continuously increases, the size of the atomic cloud σ_a will be much greater than that of the laser beam and less atoms deflected by the atomic lens, and the final transverse RMS

velocity tends asymptotically to the initial RMS velocity. This also can be seen from Eq. (23), if $\sigma_a \gg \sigma_0$, $v_y^{rms} \simeq v_0^{rms}$.

From Fig. 4 one can also observe that the minimum transverse RMS velocity is about $0.2v_0^{rms}$ for $T_0 = 0.2\mu k$ while the one is about $0.48v_0^{rms}$ for $T_0 = 0.6\mu k$. This tells us that the lower initial RMS velocity is helpful to raise the collimation efficiency, which implies that atomic lens is suitable for collimating ultracold atomic cloud rather than hot atomic cloud.

To verify the analytic result, we use the direct simulation Monte Carlo (DSMC) approach [35] to simulate the process. In the simulation the ^{87}Rb atomic cloud with initial temperature T_0 and the center velocity v_0 along z direction is placed at position L_o , after the cloud passing through the laser beam we then measure the transverse velocity spread of the atomic cloud. From Fig. 4 one notes that the analytical results agree well with the simulation ones (represented by the square symbol).

In the following text, we will discuss the vertical velocity spread of the atomic cloud. According to the law of conservation of energy, in the dipole conservative potential, the change in the kinetic energy of the atom along z direction should be equal to that along y direction

$$\Delta E_z = \Delta E_y, \quad (24)$$

Here we define the variance of velocity along z direction Δv_z . Eq. (24) becomes

$$\Delta v_z^2 + 2v_{z0}\Delta v_z = v_{y0}^2 \frac{L_o}{f} \left[\frac{L_o}{f} \exp\left(-\frac{v_{y0}^2}{\Delta v_0^2}\right) - 2 \right] \exp\left(-\frac{mv_{y0}^2}{2k_B T_0}\right) \quad (25)$$

With the previous assumption $v_{z0} \gg \Delta v_z$, Eq. (25) can be written as

$$\Delta v_z \simeq \frac{v_{y0}^2}{2v_{z0}} \frac{L_o}{f} \left[\frac{L_o}{f} \exp\left(-\frac{v_{y0}^2}{\Delta v_0^2}\right) - 2 \right] \exp\left(-\frac{mv_{y0}^2}{2k_B T_0}\right). \quad (26)$$

Finally, one can find the vertical RMS velocity of the atomic cloud

$$(v_z^{rms})^2 = A \int_{-\infty}^{\infty} (v_{z0} + \Delta v_z)^2 \exp\left(-\frac{m(v_{z0} - v_0)^2}{2k_B T_0}\right) dv_{z0} \quad (27)$$

$$(v_z^{rms})^2 = \left(\frac{1}{(2\beta + 1)^{3/2}} \frac{L_o^2}{f^2} - 2 \frac{1}{(\beta + 1)^{3/2}} \frac{L_o}{f} + 1 \right) (v_0^{rms})^2, \quad (29)$$

Obviously, under the assumption $E_0 \gg U$, the vertical RMS velocity is almost no change after the atomic cloud passing through the laser beam. We can explain this phenomenon by the fact that, compared with vertical kinetic energy, the energy transferred from transverse direction to vertical direction is so small that the corresponding vertical velocity and its width is almost not changed. The simulation result (Shown by diamond symbol in Fig. 3.) confirms the analytical prediction.

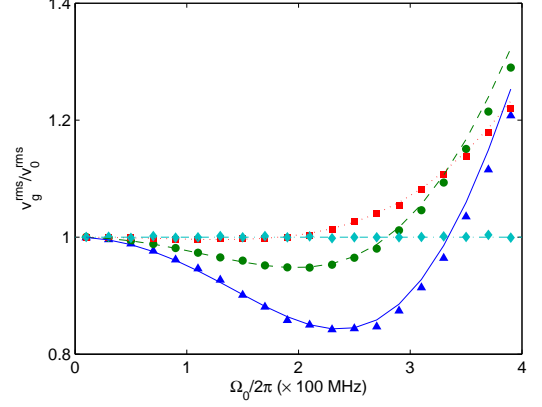


FIG. 4: (Color online) The transverse velocity spread as function of Rabi frequency. The dotted, dashed and solid lines respectively represent the transverse velocity spread of the atomic clouds when the waist widths of the laser beam are 50, 125 and 200 μm , respectively. The dash-dotted line denotes the vertical velocity spread of the atomic cloud. The symbol \blacktriangle , \blacksquare , \bullet and \blacklozenge are corresponding simulation results. In the simulation the initial temperatures, radial and velocity of the atomic cloud respectively are $T_0 = 1.0\mu k$, $R_0 = 0.1\mu\text{m}$, the initial height of the atomic cloud is $H = 3.1\text{mm}$. The parameter for the optical potential respectively are $\delta/2\pi = -50\text{GHz}$.

B. In gravity field

Next we will consider the collimation effect when an atomic cloud falls freely with a vanishing initial center velocity under the gravity. To obtain the transverse RMS velocity of the atomic cloud, we should first find the transverse velocity of it. Using the same method in previous part to find Eq. (22) one gets

$$v_{yg} = v_{y0} \left[1 - \frac{L_o}{f} \exp\left(-\frac{v_{y0}^2}{\Delta v_g^2}\right) \right], \quad (28)$$

where $\Delta v_g = \sigma_0 \sqrt{g/2H}$. So the transverse RMS velocity of the atomic cloud in the gravity is

where $\beta = \sigma_\beta^2/\sigma_0^2$ and $\sigma_\beta^2 = 4Hk_B T_0/mg$. Eq. (29) is similar with that in the uniform velocity case.

In the gravity case, $L_o/f = 2\sqrt{\pi}|U_0|/(mg\sigma_0)$, which is not dependent on the initial height of the atomic cloud but proportional to the strength of the laser beam. Fig. 5 plots v_{yg}^{rms} against Ω_0 with different waists of the laser beam. We see that the transverse RMS velocity first decreases and then increases with increasing Rabi frequency, which is similar with that in the uniform velocity case. Additionally, from Fig. 4 one can notice that

large waist of the laser beam is helpful to obtain better collimation effect. It is readily understandable that the waist of the laser beam is larger, the ratio of the size of atomic cloud to the width of the laser beam is smaller, and laser beam is more like an ideal lens, the collimating efficiency is therefore improved. The corresponding simulation results are well consistent with analytical ones.

IV. EXPERIMENTAL RESULT AND DISCUSSION

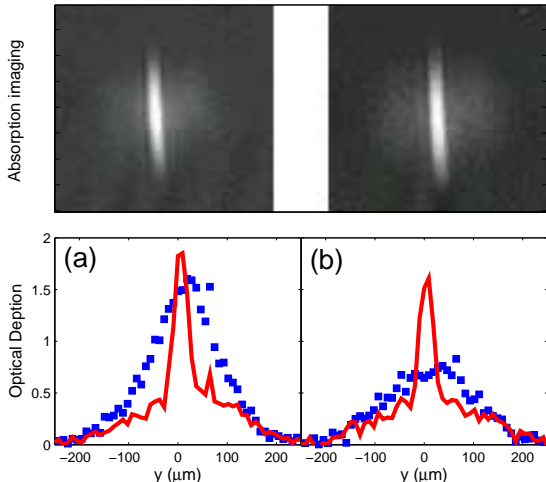


FIG. 5: (Color online) The focusing of atomic clouds by the Gaussian laser beam. Top panel is the absorption imaging of the focused atomic clouds. The bottom panel is the corresponding cross section of optical depth. The solid line denotes the the focused atomic clouds, while the symbol \blacksquare represents the reference one. The flying time t_0 is 7ms before the atomic cloud entering the laser beam. The initial temperatures of the atomic clouds are (a) 190nK and (b) 370nK respectively. Another parameters are $U_0 = 2.81 \times 10^{-29}$ J, $\sigma_0 = 35\mu\text{m}$.

Our experimental setup consists of two magneto-optical traps [32]. The atomic cloud is firstly captured in the Up-MOT and then transferred into the second ultrahigh-vacuum MOT(UHV-MOT). After the atomic number in the UHV-MOT is stable, we did optical molasses and then loaded atoms into a quadrupole-Ioffe-configuration (QUIC) trap. Evaporative cooling of the atoms was performed by rf-induced spin flips. We swept the rf frequency from 25MHz to a value of around 1.6MHz over a period of 28s. Atomic clouds with various temperatures from about $1\mu\text{K}$ to below the phase transition point were obtained by setting different rf frequencies. The cold atomic cloud then ballistically expanded after the magnetic trap was switched off. The direction of propagation of the focused Gaussian beam and the probing beam was parallel to the long axis of the QUIC trap. Therefore, the cold atomic clouds symmetrically distributed in the probing plane before traversing the Gaussian beam. We

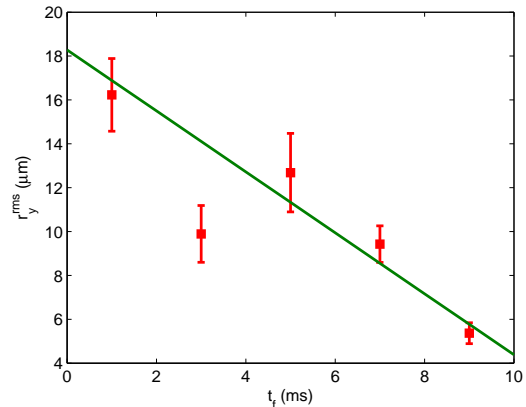


FIG. 6: (Color online) The transverse FWHM width of atomic clouds plotted against the flying time. The solid line is the analytical result. Before passing through the Gaussian beam, the atomic clouds have already flown 7 ms. Another parameters are $U_0 = 1.26 \times 10^{-29}$ J, $\sigma_0 = 17\mu\text{m}$, $T_0 = 0.071\mu\text{K}$.

acquired the distribution of atomic clouds from absorption images, as shown in Fig. 5. The Rayleigh length was about 8.5mm. Since the Rayleigh length was far greater than the scale of the atomic cloud while it was passing the light beam, we could approximate that the laser beam provided a two-dimensional Gaussian potential. When evaporative cooling was finished, we released the atomic cloud from the QUIC trap and turned on the Gaussian beam. After the atomic cloud had passed through it, we turned off the Gaussian beam and waited for several milliseconds. All information regarding the atomic cloud were derived from the absorption images.

Fig. 5 is a typical experimental result about the focusing of the atomic cloud passing through the laser beam. From absorption images and cross section of optical depth we can see that the atomic clouds are focused by the laser beam compared to the reference one. Obviously, the focusing just happened on the transverse direction, while the vertical direction remains unchanged. Owing to the finite action length of the laser beam, just part of the atomic cloud is focused. With increasing the initial temperature, the focused part is increasing. We fit the cross curves by an asymmetric bi-Gaussian to derive the Full-Width at Half-Maximum (FWHM) of the width of the focused part in the atomic clouds along transverse direction. Under the experimental parameters, the imaging time $t_i \approx 7.6\text{ms}$, the flying time $t_f = 9\text{ms}$, according to the previous analysis, the FWHM widths of the focused part should be about $8\mu\text{m}$. However, the experimental results are both of them are about $13\mu\text{m}$ and greater than the theoretical prediction, which is mainly caused by the aberration of the atom-optical lens [37, 38].

Imaging is one of important properties of atom-optical lens. If an atomic cloud with very lower initial temperature passes through the laser beam, according to Eq. (16), the FWHM width of the focused atomic cloud will

be

$$\begin{aligned} r_y^{rms} &= v_y^{rms} |t_f - t_i| \\ &= \frac{t_o}{t_i} v_0^{rms} |t_f - t_i|. \end{aligned} \quad (30)$$

Obviously, when $t_f < t_i$, the FWHM is inversely proportional to the flying time, which is plotted by solid line in Fig. 6. The experimental result is well consistent with the analytical prediction.

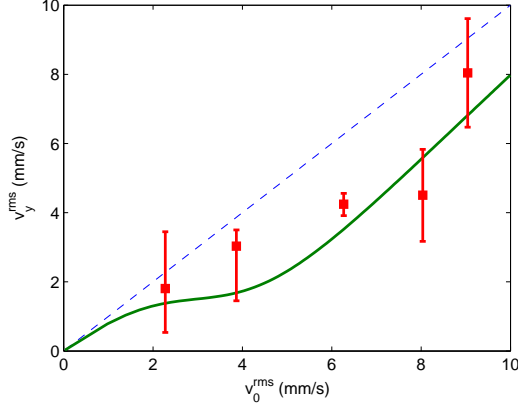


FIG. 7: (Color online) The total velocity spread against the initial one. The solid line is the analytical result. The dashed line is the reference one. Before passing through the Gaussian beam, the atomic clouds have already flown 4 ms. Another parameters are $U_0 = 2.77 \times 10^{-29}$ J, $\sigma_0 = 35 \mu\text{m}$.

We also experimentally study the collimation effect of atomic lens. The collimation effect can be measured by the final velocity spread of the atomic cloud after it passing through the Gaussian laser beam. As discussed in Ref. [32], when the initial temperature of the atomic cloud is high, only the part with lower transverse velocity is focused, other part not interacts with the laser beam. There are focused and unfocused parts in the atomic cloud after it passing through the laser beam. By measuring the RMS widths of the focused and unfocused parts in the atomic width, one can determined the total velocity spread and then measure the total collimation effect. The transverse RMS velocities of focused part and unfocused part are

$$v_f^{rms} = \frac{r_f^{rms}}{|t_f - t_i|} \quad (31)$$

and

$$v_{unf}^{rms} = \frac{r_{unf}^{rms}}{(t_f + t_o)}, \quad (32)$$

where r_f^{rms} and r_{unf}^{rms} are FWHM width of focused and unfocused parts in the atomic cloud. So the total transverse RMS velocity of the atomic cloud is

$$(v_{total}^{rms})^2 = \frac{N_f}{N} (v_f^{rms})^2 + \frac{N_{unf}}{N} (v_{unf}^{rms})^2, \quad (33)$$

where N_f , N_{unf} and N are the number of focused, unfocused and total atoms, respectively.

Fig. 7 shows the experimental result of the total transverse RMS velocity with dependence of the initial RMS velocity of the atomic cloud. Obviously, the total transverse RMS velocity is smaller than the initial one, that is to say, the atom-optical lens efficiently collimate cold atomic clouds. With the parameters experimentally available, the collimation effect is not very well when the the initial velocity spread (temperature) is lower.

V. CONCLUSION

We study the optical properties of the atomic lens induced by the far red-detuned laser beam and collimation effect of atomic cloud passing through the atomic lens, with uniform translational velocity and with vanishing initial translational velocity in gravity, respectively. Based on the atom deflection in dipole conservative potential, the object-image relation and the focal length of the atomic lens is theoretically presented. And then, the collimation effect of the atom-optical lens is theoretically studied. With the transverse RMS velocity, we find that collimation effect of the atomic cloud with lower initial RMS velocity is better than that with a high initial RMS velocity. Furthermore, theoretically speaking, the collimation by atomic lens can reach smaller divergence angle than that by transverse cooling technology due to the collimation of atomic lens without the cooling limit. Therefore the atomic lens is suitable for collimating the ultracold atomic cloud or beam. Moreover, atomic lens created by the laser beam has the advantages of small scale and flexible adjustment. It will play important role in many fields, such as integrated atom optics, atomic fountain clock. Finally we have experimentally demonstrated focusing, imaging and collimation of atomic cloud passing through the Gaussian laser beam, which are well consistent with the theoretical prediction.

This work is supported by the National Natural Science Foundation of China under Grant Nos. 10828408, 10588402, 10804115 and 10974211, National Fundamental Research Program of China under Grant Nos. 2011CB921604 and 2011CB921504.

-
- [1] C. Monroe, W. Swann, H. Robinson, and C. Wieman, Phys. Rev. Lett., **65**, 1571 (1990).
- [2] M.H. Anderson, et al., Science, **269**, 198 (1995).
- [3] T. Esslinger, I. Bloch, and T.W. Hänsch, Phys. Rev. A **58**, R2664 (1998).
- [4] P. Meystre, Atom Optics, (Springer-Verlag, New York, 2001).
- [5] C.S. Adams, M. Sigel, and J. Mynek, Phys. Rep., **240**, 143 (1994).
- [6] E.A. Cornell, C. Monroe, and C.E. Wieman, Phys. Rev. Lett., **67**, 2439 (1991).
- [7] I. Bloch, M. Köhl, M. Greiner, T.W. Hänsch, and T. Esslinger, Phys. Rev. Lett., **87**, 030401 (2001).
- [8] A.S. Arnold, C. McCormick, and M.G. Boshier, Phys. Rev. A., **65**, 031601 (2002).
- [9] R. R. Chaustowski, V. Y. F. Leung and K. G. H. Baldwin, Applied Physics B, **86**, 491 (2007)
- [10] M.J. Pritchard, A.S. Arnold, D.A. Smith, and I.G. Hughes, J. Phys. B: At. Mol. opt. Phys., **37**, 4435 (2004).
- [11] S. Choi and K. Burnett, Phys. Rev. A., **56**, 3825 (1997).
- [12] J.E. Bjorkholm, R.R. Freeman, A. Ashkin, and D.B. Pearson, Phys. Rev. Lett., **41**, 1361 (1978).
- [13] J.E. Bjorkholm, R.E. Freeman, A. Askin, and D.B. Pearson, Opt. Lett., **5**, 111 (1980).
- [14] J. Yin, W. Gao, Y. Zhu, Prog. Opt., **45**, 1197 (2003).
- [15] G.M. Gallatin, and P.L. Gould, J. Opt. Soc. Am. B, **8**, 502 (1991).
- [16] L.E. Helseth, Phys. Rev. A., **66**, 053609 (2002).
- [17] V.I. Balykin, V.S. Letokhov, Yu.B. Ovchinnikov, and A.I. Sidorov, Phys. Rev. Lett., **60**, 2137 (1988).
- [18] P.J. Martin, B.G. Oldaker, A.H. Miklich, and D.E. Pritchard, Phys. Rev. Lett., **60**, 515 (1988).
- [19] V.I. Balykin, V.S. Letokhov, and A.I. Sidorov, JETP. Lett. **43**, 217 (1986).
- [20] V.I. Balykin, V.S. Letokhov, and Yu.B. Ovchinnikov, et al., J. Mod. Opt., **35**, 17 (1988).
- [21] H. Ito, K. Yamamoto, A. Takamizawa, H. Kashiwagi, and T. Yatsui, J. Opt. A: Pure Appl. Opt., **8**, S153 (2006).
- [22] V.I. Balykin, and V.G. Minogin, Phys. Rev. A., **77**, 013601 (2008).
- [23] J.L. Cohen, B. Dubetsky, and P.R. Berman, Phys. Rev. A., **60**, 4886 (1999).
- [24] B. Rohwedder, and M. Orszag, Phys. Rev. A., **54**, 5076 (1996).
- [25] B. Dubetsky, and P.R. Berman, Phys. Rev. A., **58**, 2413 (1998).
- [26] D.R. Murray, and P. Öhberg, J. Phys. B: At. Mol. opt. Phys., **38**, 1227 (2005).
- [27] P. Barberis, and B. Rohwedder, Phys. Rev. A., **67**, 033604 (2003).
- [28] O. Steuernagel, Phys. Rev. A., **79**, 013421 (2009).
- [29] J.L. Cohen, B. Dubetsky, and P.R. Berman, Phys. Rev. A., **60**, 3982 (1999).
- [30] L. Fallani, F.S. Cataliotti, J. Catani, C. Fort, M. Modugno, M. Zawada, and M. Inguscio, Phys. Rev. Lett., **91**, 240405 (2003).
- [31] L. Pruvost, D. Marescaux, O. Houde, and H.T. Duong, Opt. Commun., **166**, 199 (1999).
- [32] S. Y. Zhou, Z. L. Duan, J. Qian, Z. Xu, Weiping Zhang, and Y. Z. Wang, Phys. Rev. A, **80**, 033411 (2009)
- [33] V. I. Balykin, V. S. Letokhov, V. G. Minogin and T. V. Zueva, Appl. Phys. B, **35**, 149 (1984).
- [34] E. Marechal, S. Guibal, J.L. Bossennec, R. Barbe, J.C. Keller, and O. Gorceix, Phys. Rev. A **59**, 4636 (1999).
- [35] G. A. Bird, *Molecular Gas Dynamics and the Direct Simulation of Gas Flow* (Clarendon, Oxford, 1994).
- [36] Y.Z. Wang, S.Y. Zhou, Q. Long, S. Y. Zhou, H. X. Fu, Chin. Phys. Lett., **20**, 799 (2003).
- [37] J.J. McGlelland and M.R. Scheinfein, J. Opt. Soc. Am. B, **8**, 1974 (1991).
- [38] R. Arun, Offir Cohen, and I. Sh. Averbukh, Phys. Rev. A **81**, 063809 (2010).